Seasonal Distributions of Fine Aerosol Sulfate in the North American Arctic Basin during TOPSE

Eric Scheuer, Robert W. Talbot, Jack E. Dibb, Garry K. Seid, Linsey DeBell

Institute for the Study of Earth, Oceans and Space, University of New Hampshire, Durham, NH

Barry Lefer

Atmospheric Chemistry Division, NCAR

corresponding author: Eric Scheuer, eric.scheuer@unh.edu, (603) 862-2284, fax (603) 862-0188

For submission to the special issue of JGR Atmospheres on TOPSE

28 September 2001

Abstract.

We used the mist chamber/ion chromatography technique to quantify fine aerosol $SO_4^=$ (< 2.7 μm) in the Arctic during the Tropospheric Ozone Production about the Spring Equinox Experiment (TOPSE) with about 2.5 minute time resolution. The results from this technique compared well with the bulk aerosol technique, which is not unexpected since most sulfate mass in the Arctic is associated with particles with diameters smaller than 0.5 μm. The seasonal evolution of fine aerosol sulfate in the Arctic troposphere during TOPSE was consistent with the phenomenon of Arctic haze. Arctic haze has been described as pollution transported meridionally along stable isentropes into the Arctic in geographically broad but vertically narrow bands. These layers become more prevalent at higher altitudes, as the season progresses toward summer and the relevant isentropes are not held so close to the surface. Mean mixing ratios during TOPSE in February below 1000 meters were elevated (112 pptv) and highly variable (between 28 and 290 pptv), but were significantly lower at higher altitudes (about 40 pptv). As the season progressed, elevated mixing ratios, and higher variability was observed at higher altitudes, up to 7 km. In May, mixing ratios at the lowest altitudes declined, but still remained higher than in February at all altitudes. The high variability in our measurements likely reflects the vertical heterogeneity of the wintertime Arctic atmosphere as the airborne sampling platform passed in and out of these layers. It

is presumed that mixing ratios and variability will continue to decline at all altitudes into the summer as wet deposition processes become important.

1. Introduction

Accumulation of aerosols and anthropogenic pollutant gasses in the troposphere during the Arctic wintertime is well documented [*Rahn*, 1981, *Barrie*, 1986]. The slow transformation and removal processes due to cold sub-zero temperatures, absence of wet precipitation, and low levels of solar radiation [*Barrie*, 1986] coupled with a slow, low-level, long-range northward meridional transport of Eurasian mid-latitudinal pollutants into the Arctic lead to annual wintertime events which have become to be known as Arctic haze. This visual haze is largely due to aerosol light scattering properties of accumulation mode particles [*Brock et al*., 1989], which exhibit dominant presence around the 0.01-0.5 μm effective diameter range [*Blanchet and List*, 1983]. The hazes have been shown to be primarily of anthropogenic origin [*Radke and Hobbs*, 1984] with aerosol $SO_4^=$ constituting more than half of the total aerosol mass [*Shaw*, 1989]. Most of this $SO_4^=$ mass is derived from anthropogenic emissions of SO_2 rather than primary particulate emissions [*Barrie and Hoff*, 1984]. Much of these emissions are believed to have originated from Europe and Russia [*Rahn*, 1981] and been transported isentropically into the Arctic in multi-day long pulses as low pressure systems run up against the quasi-stationary Siberian high [*Barrie*, 1986].

Arctic Haze is believed to be influential on radiative budgets, snowpack albedo, snowpack chemical composition, and microphysical properties of Arctic clouds [*Brock et*

al., 1990]. Measurements of $SO_4^=$ aerosols in the Arctic have often been limited to geographically fixed locations in the Arctic over the course of a season. These data tend to be lacking information on spatial variability, both horizontally and vertically. Intensive airborne measurement campaigns conducted in both the summer (ABLE 3A-3B, 1988, 1990) and winter (AGASP I-IV, 1983, 1986, 1989, and 1991) into the Arctic have reported only a limited number of aerosol $SO_4^=$ measurements due to relatively long sample integration times inherent with filter collection techniques.

In the early months of 2000, the heavily instrumented NSF/NCAR C-130 research aircraft conducted a series of trips into the Arctic beginning on February 4, 2000 and continuing until May 23, 2000. This campaign was called the Tropospheric Ozone Production about the Spring Equinox Experiment, or TOPSE. The primary objective of TOPSE was to study Arctic ozone production, loss and transport with a focus on the commonly observed springtime Arctic ozone maximum. It consisted of seven trips (42 total flights) from Boulder, Colorado (38^oN) into the high Arctic environment (86^oN). *Atlas et. al*. (this issue) provides an instrument payload description and detailed objectives of the flights conducted during TOPSE.

This field campaign provided an excellent opportunity to use the University of New Hampshire's dual mist chamber/ion chromatograph technique to examine the seasonal and vertical distributions of fine aerosol $SO_4^=$ in the Arctic. This technique was developed for the measurement of soluble gases such as HNO_3, CH_3COOH, HCOOH [*Talbot*, 1999], SO_2 [*Klemm and Talbot*, 1991], HCl [*Keene*, 1993], and HONO [*Dibb*, in press]. Experiments during prior intensive aircraft campaigns have demonstrated that with only minor modifications, measurements of fine soluble aerosols were possible.

This technique is well suited for $SO_4^=$ because a significant mass fraction is generally in the accumulation mode. Previously, soluble aerosol sampling has been restricted to Teflon filter exposure and subsequent solvent/water extraction. The Teflon filter technique, although yielding more potential analytes, suffers from long integration times, generally between 15 and 30 minutes. During the nearly 4-month period, 3820 samples were successfully collected using the mist chamber/ion chromatography technique with an average integrated collection time of 2.5 minutes. Analysis was performed in near-real time with detection limits as low as 4 parts per trillion by volume (pptv). To date, this was the most extensive $SO_4^=$ aerosol data set collected from an airborne platform.

Twenty bulk aerosol measurements were made during TOPSE using the NCAR-RAF Small Community Aerosol Inlet (SCAI) and Teflon filters. These measurements were made primarily to help speciate detectable, but unexpected, amounts of soluble Br^- measured in many low altitude mist chamber samples. Aerosol $SO_4^=$ was also detected and quantified in these samples, providing some measure of comparison to the mist chamber samples.

2. Methods

2.1 Sampling and Analysis

A schematic representation of the University of New Hampshire mist chamber/ion chromatograph is seen in Figure 1. Soluble aerosol species were collected in deionized water using two mist chambers [*Talbot,* 1999] operating alternately between collection and analysis cycles. The mist chambers were connected to a sample manifold protruding from the aircraft about 25 centimeters, far enough to be in the free air stream and

minimally affected by aircraft boundary layer effects. A 0.5 cm outer diameter inlet was positioned 90^o to the airflow streamline over the aircraft, but was cut at a forward facing 45^o angle. This 45^o angle ensured that aerosol collected were small enough to make the 90^o turn into the inlet, while larger particles were impacted on the inside face of the 45^o cut. This design is believed to have excluded a majority of less radiatively important super-micron aerosols, commonly associated with sea salt and coarse mode dust. Based on particle stopping distance calculations taken from *Hinds* [1982] eqn.5.3 and 5.19, and an estimated average cruise speed of 129 meters per second (250 KTAS), the median cutoff particle size sampled by our inlet is estimated to be about 2.7 μm. Although this is a slightly larger cutoff than was desired, it still excludes a large percentage of coarse mode particles. Indeed, the bulk of the mass distribution of $SO_4^=$ has been shown to be centered on 0.3 μm [*Blanchet*, 1989], a size which we believe to have sampled effectively. A more rigorous inlet design, although desirable, was not attempted due to time, financial and airworthiness constraints coupled with the need to optimize passing of nitric acid (the species of primary interest to this instrument) in the same inlet.

Chemical analysis of the samples collected by the mist chambers was conducted in near real-time using ion chromatography. The aqueous samples were removed from the mist chamber by computer controlled syringe pumps (Kloehn 50300) and injected into custom fabricated ion chromatographs employing sample preconcentration (Dionex TAC-LP1). Separation was achieved using a helium purged carbonate/bicarbonate eluent and Dionex AS4A analytical columns. Background conductivity was suppressed using Dionex ASRS-Ultra suppressors. Detection of Cl^-, Br^-, NO_3^-, SO_3^- and $SO_4^=$ was accomplished using a Dionex CD-20 conductivity detector equipped with a DS-3

temperature controlled cell. Digitized data was then sent to a data acquisition computer using standard ethernet communications where post processing took place. An internal spike of known aqueous concentration of phosphate into the mist chamber and subsequent analysis was used to track any evaporative losses of water from the mist chamber during sampling. Two independent systems operated in tandem, which allowed for continuous sampling with an average 2.5-minute time resolution. It is important to note, that unlike conventional filter techniques, all sample and fluid handling was closed and isolated from the aircraft cabin ambient air, preventing contamination.

3. Results

3.1 Filter intercomparisons - previous missions

During the 1999 NASA aircraft campaign Pacific Exploratory Mission – Tropics B (PEM-Tropics B) in the South Pacific, we collected aerosol $SO_4^=$ data using the standard Teflon filter technique and the mist chamber/ion-chromatography technique simultaneously. Although most aerosol $SO_4^=$ mass is in accumulation size mode, there can be a significant fraction associated with sea-salt or crustal dust that is in the much larger coarse mode. Since the standard Teflon filter technique was designed for bulk aerosol sampling rather than a size selected fraction, some correction to make the data comparable was necessary. Most coarse particle $SO_4^=$ is usually associated with sea-salt, especially over the ocean. This makes a simple sea-salt correction to the total $SO_4^=$ an acceptable method to approximate the fine aerosol $SO_4^=$ (or non-sea salt) component. Examples of the comparison between fine aerosol $SO_4^=$ (mist chamber/ion chromatograph) and non-sea salt $SO_4^=$ (Teflon filters) from both the NASA DC-8 and the

NASA P3-B research aircraft are presented in Figure 2. Agreement between the two techniques was very good. The mist chamber/ion chromatography technique, however, exhibited much better time resolution than the Teflon Filter technique. This can be especially important during aircraft ascents and descents where a discrete sample represents a non-uniform altitude. Minimizing sample integration times becomes important in minimizing the vertical extent over which a sample is integrated. Filter samples are often not collected during ascents and descents because of this averaging issue.

3.2 Filter intercomparisons during TOPSE

The NCAR Small Community Aerosol Inlet (SCAI) with a University of New Hampshire modified curved leading edge nozzle was employed during TOPSE to sample aerosol radionuclides [*Dibb*, this issue]. This inlet was also used to collect a limited number of bulk aerosol samples isokinetically on Teflon filters at low altitudes. These samples were collected in order to facilitate speciation of soluble bromide observed in the mist chamber/ion chromatography analysis, however, aerosol $SO_4^=$ was also quantified in these samples. This provided a basis for comparison of TOPSE mist chamber/ion chromatography samples to bulk aerosol filer samples. Figure 3 shows excellent agreement in the $SO_4^=$ data when measured using the two techniques. The variability in the mist chamber data represents the standard deviation of the mean mixing ratio measured by the mist chamber during the time period that a bulk filter sample was being collected. All of the bulk aerosol filters collected during TOPSE were at very low altitudes, during events where soluble bromide was detectable in the mist chamber. With

the increased presence of a super-micron fraction and sea-salt associated $SO_4^=$ at lower altitudes, it is not unexpected that the bulk aerosol data has a tendency to show slightly higher mixing ratios than the mist chamber data. Sea-salt is not believed to be a significant issue with any of our TOPSE samples, however, since most of our low altitude samples were collected over pack ice, and not open water. Intercomparison data from a previous airborne sampling campaign (NASA PEM-Tropics B) suggest that agreement is even better at higher altitudes where $SO_4^=$ is almost exclusively on fine aerosols uninfluenced by sea-salt.

3.3 Fine Aerosol $SO_4^=$ measured during TOPSE

A summary of the fine aerosol $SO_4^=$ data collected during TOPSE is presented in Table 1. The Table is restricted to latitudes greater than 50^{o}N, since data collected south of 50^{o}N were collected during transit flights to the primary study region. In order to examine the seasonal evolution of fine aerosol $SO_4^=$ in the Arctic, the data were summarized by trip and grouped into discrete 1000-meter altitude bins in the latitude range of 50^{o}N-86^{o}N. Mixing ratios as high as 1766 pptv and as low as 4 pptv were observed during TOPSE (Table 1). The lowest values were generally observed during the first trip in early February. This trip also had the lowest variability in most altitude bins. The highest values were observed during the sixth trip in late April, which also exhibited the greatest variability.

Our range of data is consistent with data presented by Lazrus and Ferek (1984) from the 1983 AGASP airborne sampling campaign. They report $SO_4^=$ concentrations in the Arctic as low as 7.3 neq/m^3 (82 pptv) and as high as 110 neq/m^3 (1233 pptv). Their

samples, however, represent much longer periods of integration, and are less likely to represent a completely homogenous sample. That is, each one of their samples is more prone to have passed in and out of haze layers. This explains the smaller range of mixing ratios reported. Their highest value presented is reported to have been collected while flying in a continuous haze layer and may reflect a more homogeneous sample. Indeed, their highest mixing ratio reported is very similar to what we observed.

The frequency distribution of our raw data collected is normally distributed about a mean. This can be explained by an abundance of cleaner air riddled with thin, highly polluted, layers. That is, since the polluted layers can be strongly delineated from the cleaner air, there appeared to be an absence of more moderate transition layers. As with many environmental data sets, the data are highly skewed by less frequent but very high values. Arithmetic means are only representative of data that is at least close to normally distributed since they can be very sensitive to very large values. This makes using arithmetic means for our $SO_4^=$ data bins very misleading. Using medians can have the opposite effect, and can lack sensitivity to real data that is far from the mean. To address this problem, we use geometric means since the data are more nearly log-normally distributed. This statistical tool addresses more of the real variability within the data set without placing emphasis on unusually high or low values. It also allows us to visualize real variability in the form of log-normally transformed standard deviations; presented graphically as unequal length error bars in Figure 4.

During the first trip in early February, fine aerosol $SO_4^=$ mixing ratios were relatively low and not highly variable above 1000 meters (Figure 4, top panel). Below 1000 meters the range of mixing ratios was significantly higher and yielded a geometric

mean of 110 pptv. This mean was more than two-fold higher than in any other altitude bin during this trip. Interestingly, Ridley et al (this issue) report a rarity of pollution events at very low altitude. $SO_4^=$ mixing ratios were, however, noticeably enhanced all the way to the lowest altitudes surveyed during TOPSE throughout the campaign. Barrie (1986) reported data summarized by Rahn and Heidman (1981) noting that winter/spring pollution aerosols measured from a ground based Arctic aerosol sampling network averaged 2 µg/m3 $SO_4^=$ (466 pptv). This is consistent with our observations of near-surface $SO_4^=$ enhancements.

During the second trip (late February), mean mixing ratios in the two lowest bins were almost double what was observed during the first trip, but mean mixing ratios above 2000 meters remained around 50 pptv and were not highly variable. This trend of increasing mean mixing ratios at increasingly higher altitudes as the season progresses continued into trip 3 in early March. Mean mixing ratios below 5000 meters all appeared to be enhanced and increasingly variable with respect to earlier trips. There was also a gradient of about 70 pptv in mean mixing ratios (100 to 170 pptv) between the 2000 to 3000 meter bin and below 1000 meters.

Mean mixing ratios were above 100 pptv in all altitude bins and above about 225 pptv below 2000 meters by trip 4 in late March. The steepest gradient in $SO_4^=$ mean mixing ratio was no longer below 1000 meters, but rather between 1000 and 3000 meters. The trend of increasing mean mixing ratios in all altitude bins from trip to trip but decreasing mean mixing ratios with altitude began to show marked change during trip 5 in early April. Mean mixing ratios below 2000 meters were lower than on the previous trip while mean mixing ratios above 2000 meters continued to increase, albeit less

dramatically. During the last two trips, fine aerosol sulfate mean mixing ratios generally continued to decrease below 3000 meters and increase above 4000 meters. By the end of the data collection phase of TOPSE, $SO_4^=$ mean mixing ratios showed no obvious altitude gradient and were greater than 3-fold higher at all altitudes above 1000 meters than they were in early February (about 30 percent higher below 1000 meters).

Talbot et al, [1992] reported aerosol sulfate mixing ratios averaging 29 pptv in the boundary layer and 65 pptv in the free troposphere during the ABLE 3A (1988) summer campaign in the Arctic. This suggests that $SO_4^=$ mixing ratios in the high Arctic should continue declining through late spring into the summer, possibly exhibiting a gradient inverse to that noted in the earlier TOPSE trips. This decrease must happen rapidly during the month of June, and may be related to the onset of warmer temperatures and liquid precipitation.

The seasonal evolution of aerosol $SO_4^=$ in the Arctic is shown in a different format in Figure 5. Mean mixing ratios of $SO_4^=$ below 2000 meters increased during early February until the end of March, reaching a mean mixing ratio maximum of about 220 pptv. During April and May mean mixing ratios then declined to about 150 pptv. In the middle troposphere (2000-5000 meters), mixing ratios continued to increase until the end of March reaching a mean mixing ratio peak of 200 pptv. In the upper Arctic troposphere, mean mixing ratios appeared to still be increasing at the conclusion of the sampling campaign, but had not exceeded levels in the lower and middle troposphere (which were already declining from peak values). The sharp decreasing trends in mean mixing ratios in the lower and middle troposphere coupled with the still increasing or flat

gradients in the upper troposphere would produce the summertime inverse gradient observed by *Talbot et al*. [1992].

To examine latitudinal trends in aerosol $SO_4^=$ data collected during TOPSE, we binned data into two seasons (winter and spring) and three altitude bins (below 2000 meters, 2000-5000 meters, and above 5000 meters). All samples collected north of 50°N were plotted (Figure 6) to demonstrate the variability that characterized the Arctic troposphere. This extreme variability is the result of haze layers. Samples in a given column of air may represent either a clean or a polluted layer or some combination of both. Mean mixing ratios appear to increase with latitude at all altitudes in both winter and spring. More notably, however, is sharp gradient in minimum values measured above around 70°N. This is especially evident in the lower troposphere in both the spring and winter. This trend in elevated minimum mixing ratios is also seen at higher altitudes, but the gradient is less steep. It does, however, continue to lower latitudes. This is consistent with and a nice illustration of the 7-8 kilometer deep "polar dome" described by *Barrie* [1986] and *Shaw and Khalil* [1989].

4. Discussion

The seasonal trend in vertical aerosol $SO_4^=$ distribution during TOPSE is clear in Figure 4. During early February, significant enhancements in aerosol $SO_4^=$ appear to be strongly confined near the surface. Long-range transport from the northern Eurasian continent along low level, sinking isentropes is likely most responsible for this observation. As the season progresses from winter to spring, this phenomenon of long-range isentropic transport begins to ascend vertically. Evidence that the polluted parcels

of air are confined to near the surface disappears as dramatically enhanced mixing ratios are observed at higher altitudes. We believe that, even the late winter, vertical mixing is a small or non-existent component of the observed enhancement at higher elevations. Mixing of low-level air with the overlying free troposphere is inhibited by a persistent low-level inversion [*Kahl*, 1990]. Stable inversions can last for several weeks essentially decoupling the lower troposphere from higher altitudes [*Bradley et al*., 1992]. Elevated mixing ratios at higher and higher altitudes as the season progresses must be explained by transport into the Arctic along vertically higher isentropes tracing back to warmer and warmer source regions in northern Eurasia.

During early April, below 3000 meters, levels of $SO_4^=$ enhancement began to decline. An increase in inversion base depths and decrease in inversion persistence probabilities [*Kahl et al*., 1992] hint that solar surface heating may be beginning to stir up the lowest levels of the atmosphere while more stable isentropic transport can continue at higher altitudes. Removal processes, dominated by wet deposition [*Barrie*, 1985], become increasingly important and decrease mixing ratios at lower altitudes. By the end of May, surface mixing ratios of fine aerosol $SO_4^=$ are almost half of the maximum observed in March. Mixing ratios also appear to be beginning to decrease at higher altitudes. This is consistent with the much lower values observed at all altitudes during summer months by *Talbot et al*. [1992].

The high variability observed, especially as mean mixing ratios increase (Figure 4), indicate that $SO_4^=$ aerosol mixing ratios in the Arctic winter are far from homogeneous. Mixing ratios during the late February trip (trip 2) in the 1000-2000 meter altitude bin were observed to be as low as 23 pptv and as high as 1766. This is consistent

with multiple narrow haze bands covering between 20-200 kilometers [*Radke et. al.*, 1984], and often between tens of meters to 1 kilometer thick, [*Brock et al.*, 1989], streaming slowly into the Arctic environment. Individual altitude bins of data presented here probably incorporate both cleaner and more polluted layers, leading to high variability within the bins. The observations of increasing $SO_4^=$ mean mixing ratios in an altitude bin during the winter can be attributed to more frequent occurrences of these narrow polluted layers within the bin region.

5. Conclusion.

The mist chamber/ion chromatograph is shown to be an effective tool for the measurement of fine aerosol $SO_4^=$ aboard an aircraft platform. During TOPSE, we collected an extensive fine aerosol $SO_4^=$ data set. These measurements paint a four month long picture of the vertical distributions in the Arctic. Small-scale variability and poorly understood frequencies of haze layers, however, makes estimation of total aerosol burdens difficult [*Brock et al.*, 1990]. The slow transport, and lack of major chemical transformations, however, does allow us to treat the approximately weeklong measurement campaigns as synoptic snapshots of the Arctic environment. It is shown that $SO_4^=$ aerosols begin to build up at very low altitudes during the winter. The altitude at which the buildup is most pronounced tended to migrate to higher altitudes as the season progressed toward spring. In spring, $SO_4^=$ aerosols began to clean up at lower altitudes first, progressing upward. It is possible that much of the fine detail of the Arctic air is lost in the averaging and temporal gaps in the data. Follow-up investigations into the frequency, distribution, and spatial variability of Arctic pollution layers could help

provide better information into the extent and magnitude of these layer as well as help better explain the extreme heterogeneity observed.

Acknowledgements.

We would like to express our sincere appreciation to the National Science Foundation (NSF) Office of Polar Programs (OPP) for supporting our research program through the National Center for Atmospheric Research (NCAR). We would also like to acknowledge Eliot Atlas with support from the Research Aviation Facility (RAF) for level-headedly and successfully leading us through what proved to be a very challenging environment.

References.

Atlas, E., et al., The TOPSE experiment: Introduction.

Barrie, L. A., Atmospheric Particles: Their physical and chemical characteristics, and deposition processes relevant to the chemical composition of glaciers, *Annals of Glaciology, 7,* 1985.

Barrie, L.A. and R.M. Hoff, Five years of air chemistry observation in the Canadian Arctic, *Atmos. Environ., 19,* 1995-2010, 1985.

Barrie, L.A., Arctic air pollution: An overview of current knowledge, *Atmos. Environ., 20,* 643-663, 1986.

Blanchet, J. and R. List, Estimation of optical properties of arctic haze using a numerical model, *Atmosphere-Ocean, 21*, 444-465, 1983.

Blanchet, J., Toward estimation of climatic effects due to arctic aerosols, *Atmos. Environ.*, 23, 2609-2625, 1989.

Bradley, R. S., F.T. Keimig, H.F. Diaz, Climatology of surface-based inversions in the North American Arctic, *J. Geophys. Res.*, 97, 15,699-15,712, 1992.

Brock, C.A., L.F. Radke, J.H. Lyons, and P.V. Hobbs, Arctic hazes in summer over Greenland and the North American Arctic. I: Incidence and origins, *J. Atmos. Chem., 9*, 129-148, 1989.

Brock, C.A., L.F. Radke, and P.V. Hobbs, Sulfur in particles in arctic hazes derived from airborne in situ and lidar measurements, *J. Geophys. Res., 95*, 22,369-22,387, 1990.

Dibb, J.E., R.W. Talbot, E. Scheuer, G. Seid, and L. DeBell, Stratospheric Influence on the Northern North American Free Troposphere during TOPSE: 7Be as a Stratospheric Tracer, *J. Geophys. Res., this issue.*

Dibb, J.E., and M. Arsenault, Fast Nitrogen Oxide Photochemistry in Summit, Greenland Snow, *Atmos. Environ*., in press.

Hinds, W.C. Acceleration and curvilinear particle motion, *Aerosol Technology*, pp. 105-110, John Wiley & Sons, Inc., New York, 1982.

Kahl, J.D., Characteristics of the low-level temperature inversion along the Alaskan Arctic coast, *Int. J. Climatol.*, 10, 537-548, 1990.

Kahl, J.D., M.C. Serreze, and R.C. Schnell, Tropospheric low-level temperature inversions in the Canadian Arctic, *Atmosphere-Ocean, 30*, 511-529, 1992.

Keene, W.C., J.R. Maben, A.P.P Pszenny, and J.N. Galloway, Measurement technique for inorganic chlorine gases in the marine boundary layer, *Environ. Sci. and Tech*., 27, 1993.

Klemm, O., and R.W. Talbot, A sensitive method for measuring atmospheric concentrations of sulfur dioxide, *J. Atmos. Chem*.,13, 325-342, 1991.

Lazrus, A.L., and R.J. Ferek, Acidic sulfate particles in the winter arctic atmosphere, *Geophys. Res. Lett*., 11, 417-419, 1984

Radke, F.L., and P.V. Hobbs, Airborne observations of arctic aerosols. III: Origins and effects of airmasses, *Geophys. Res. Lett.*, 11, 401-404, 1984.

Radke, F.L., J.H. Lyons, D.A. Hegg, P.V. Hobbs, and I.H. Bailey, Airborne observations of arctic aerosols. I: Characteristics of arctic haze, *Geophys. Res. Lett.*,, *11*, 393-396, 1984.

Rahn, K.A. and R.J. McCaffrey, Long-range transport of pollution aerosol to the Arctic: A problem without boarders, paper presented at the WMO Symp. On the Long Range Transport of Pollutants and its Relation the General Circulation Including Stratospheric/Tropospheric Exchange Processes, pp. 25-35, Sofia, 1-5 October 1979. WMO No. 538, 1979.

Rahn, K.A. and N.Z. Heidman, Progress in Arctic air chemistry, 1977-1980: a comparison of the first and second symposia, *Atmos. Environ*., 15, 1345-1348

Ridley B., E. Atlas, D. Montzka, E. Browell, C. Cantrell, D. Blake, N. Blake, M. Coffey, R. Cohen, R. DeYoung, J. Dibb, F. Eisele, F. Flocke, A. Fried, F. Grahek, W. Grant, J. Hair, J. Hannigan, B. Heikes, B. Lefer, L. Mauldin, R. Shetter, J. Snow, R. Talbot, J. Thornton, J. Walega, A. Weinheimer, Ozone depletion events observed in the high latitude surface layer during the TOPSE aircraft program, *J. Geophys. Res., this issue.*

Shaw, G.E., and M.A.K. Khalil, Arctic haze, *The handbook of environmental chemistry*, vol. 4, edited by O. Hutzinger, pp. 89-91, Springer-Verlag, Berlin Heidelberg, 1989.

Talbot, R.W., A.S. Vijgen, R.C. Harriss, Soluble Species in the arctic summer troposphere: acidic gases, aerosols, and precipitation, *J. Geophys. Res., 97*, 16,531-16,543, 1992.

Talbot, R.W., J.E. Dibb, E.M. Scheuer, Y. Kondo, M. Koike, H.B. Singh, L.B. Salas, Y. Fukui, J.O. Ballenthin, R.F. Meads, T.M. Miller, D.E. Hunton, A.A. Viggiano, D.R. Blake, N.J. Blake, E. Atlas, F. Flocke, D.J. Jacob, and L. Jaegle, Reactive nitrogen budget during the SONEX mission, *Geophys. Res. Lett*., 20, 3057-3060.

Table 1. Summary of Fine Aerosol Sulfate, North of 50-degree latitude, Binned by Trip and Altitude

		Sample Count	Median (pptv)	Geometric Mean (pptv)	Minimum (pptv)	Maximum (pptv)
Trip 1				*February 4-9 (Flights 5-8)*		
	<1000 meters	31	124	112	28	290
	1000-2000 meters	11	51	54	20	130
	2000-3000 meters	21	58	61	18	188
	3000-4000 meters	21	43	47	20	124
	4000-5000 meters	17	43	41	16	131
	5000-6000 meters	69	23	25	6	235
	6000-7000 meters	10	23	19	12	25
	>7000 meters	2	32	31	25	39
Trip 2				*February 21-27 (Flights 9-13)*		
	<1000 meters	59	165	155	48	406
	1000-2000 meters	52	99	97	23	1766
	2000-3000 meters	39	53	51	16	126
	3000-4000 meters	29	59	49	12	132
	4000-5000 meters	40	69	57	14	140
	5000-6000 meters	113	50	50	18	150
	6000-7000 meters	20	45	50	22	313
	>7000 meters	28	39	44	21	103
Trip 3				*March 5-8 (Flights 14-17)*		
	<1000 meters	34	171	168	98	313
	1000-2000 meters	14	117	142	44	552
	2000-3000 meters	24	133	105	4	530
	3000-4000 meters	13	117	83	8	543
	4000-5000 meters	21	86	101	23	337
	5000-6000 meters	35	50	46	8	189
	6000-7000 meters	37	27	30	9	214
	>7000 meters	15	43	37	12	117
Trip 4				*March 19-26 (Flights 18-23)*		
	<1000 meters	85	206	225	116	667
	1000-2000 meters	58	242	219	19	540
	2000-3000 meters	69	211	158	40	597
	3000-4000 meters	40	133	129	34	446
	4000-5000 meters	76	130	125	33	498
	5000-6000 meters	110	126	109	47	473
	6000-7000 meters	40	104	109	46	242
	>7000 meters	51	116	118	49	268
Trip 5				*April 2-7 (Flights 24-30)*		
	<1000 meters	85	219	209	95	598
	1000-2000 meters	43	212	217	76	504
	2000-3000 meters	33	243	221	85	400
	3000-4000 meters	33	200	194	87	364
	4000-5000 meters	93	183	176	73	407
	5000-6000 meters	110	129	122	43	324
	6000-7000 meters	79	122	120	63	307
	>7000 meters	26	131	136	59	313
Trip 6				*April 23-30 (Flights 31-36)*		
	<1000 meters	97	223	184	26	628
	1000-2000 meters	48	189	208	78	597
	2000-3000 meters	68	236	237	84	784
	3000-4000 meters	40	191	171	33	842
	4000-5000 meters	65	199	173	4	684
	5000-6000 meters	168	157	140	57	1160
	6000-7000 meters	25	172	199	69	698
	>7000 meters	59	110	120	21	470
Trip 7				*May 15-23 (Flights 37-42)*		
	<1000 meters	70	173	149	21	322
	1000-2000 meters	64	170	162	20	722
	2000-3000 meters	45	187	143	10	788
	3000-4000 meters	62	170	153	27	374
	4000-5000 meters	61	175	157	36	417
	5000-6000 meters	179	171	160	32	487
	6000-7000 meters	58	128	124	30	390
	>7000 meters	24	162	143	59	400

The geometric mean (M) commonly used for log-normally distributed data. It is the n^{th} root of the product of the values in a given bin. [$M_{(x)}= (x_1x_2\ldots x_n)^{1/n}$].

Figure 1. Schematic diagram of the two-channel mist chamber/ion chromatograph used during TOPSE.

Figure 2. Example intercomparisions of non-sea-salt $SO_4^=$ mixing ratios from filter samples and fine aerosol $SO_4^=$ from the mist chamber technique on different aircraft during PEM-Tropics B. In the top panel time-series plots, the length of the horizontal bars reflects filter exposure intervals. Mist chamber derived values are plotted at sample mid-point. The lower panels are scatter plots with least-squares regressions. For comparison, the dashed line is a 1:1 slope. Mixing ratios determined by the mist chamber technique (vertical axis) are averaged over the collection period of each filter (horizontal axis). Vertical error bars represent 1 standard deviation of mist chamber mixing ratios.

Figure 3. Intercomparision of the mist chamber/ion chromatograph technique to Teflon filter bulk aerosol $SO_4^=$ samples from TOPSE during periods of collection of the bulk aerosol samples. There were an average of 6 mist chamber samples collected for each of the approximately 15 minute bulk filter sample.

Figure 4. Vertical distributions of geometric mean mixing ratios between 50 and 85 north latitude. Error bars represent 1 standard deviation about the geometric mean and are therefore asymmetric. They represent a measure of variability of mixing ratios observed (about 68%) and not error.

Figure 5. Seasonal progression of geometric mean mixing ratios of fine aerosol $SO_4^=$ in three altitude bins.

Figure 6. Latitudinal distributions of fine aerosol $SO_4^=$ during winter and spring in 3 altitude bins. Data shown are discrete measurements made north of 50^oN.

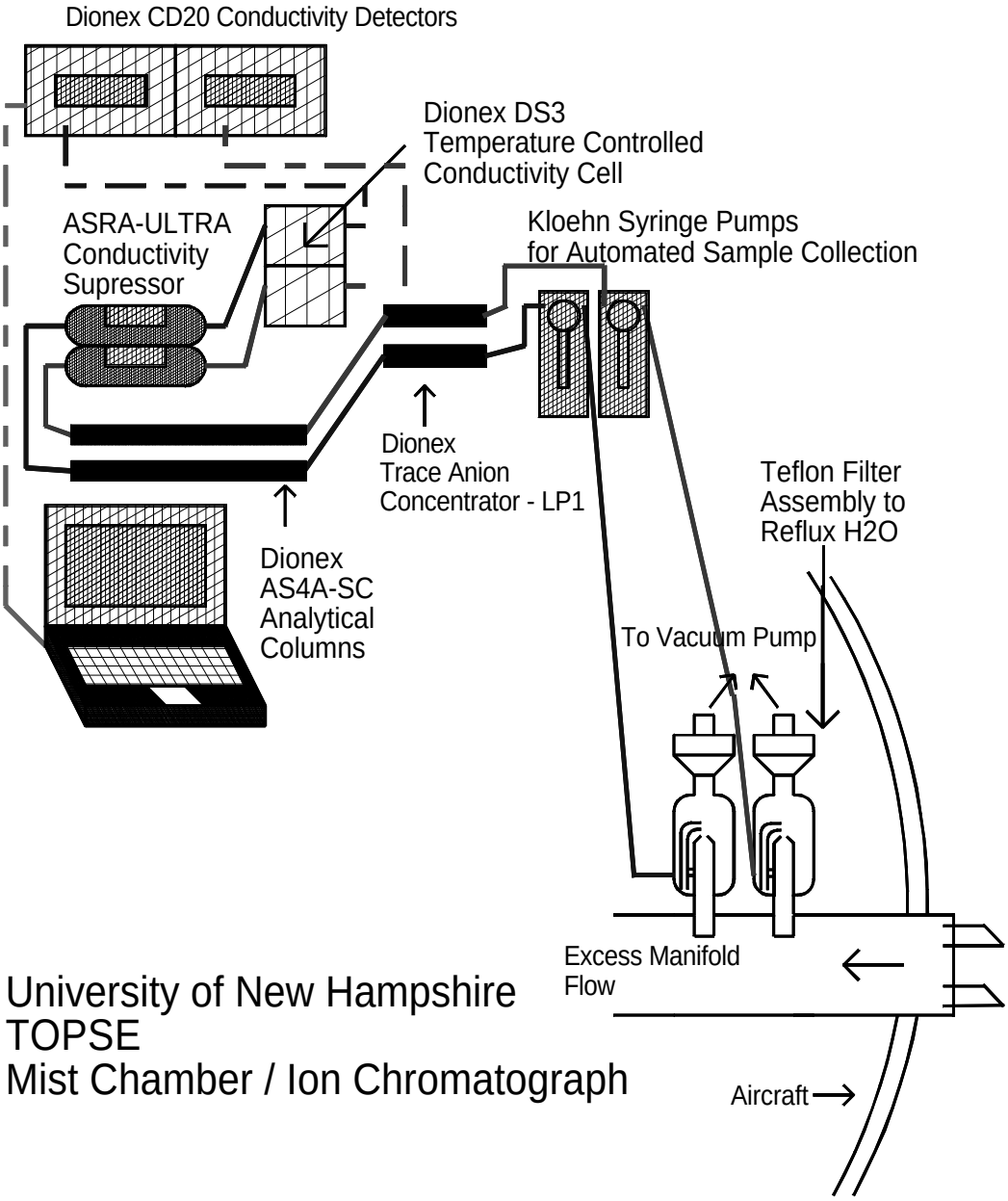
Dionex CD20 Conductivity Detectors
Dionex DS3
Temperature Controlled
Conductivity Cell
ASRA-ULTRA
Conductivity
Supressor
Kloehn Syringe Pumps
for Automated Sample Collection
Dionex
Trace Anion
Concentrator - LP1
Teflon Filter
Assembly to
Reflux H2O
Dionex
AS4A-SC
Analytical
Columns
To Vacuum Pump
Excess Manifold
Flow
Aircraft
University of New Hampshire
TOPSE
Mist Chamber / Ion Chromatograph

Figure 1.

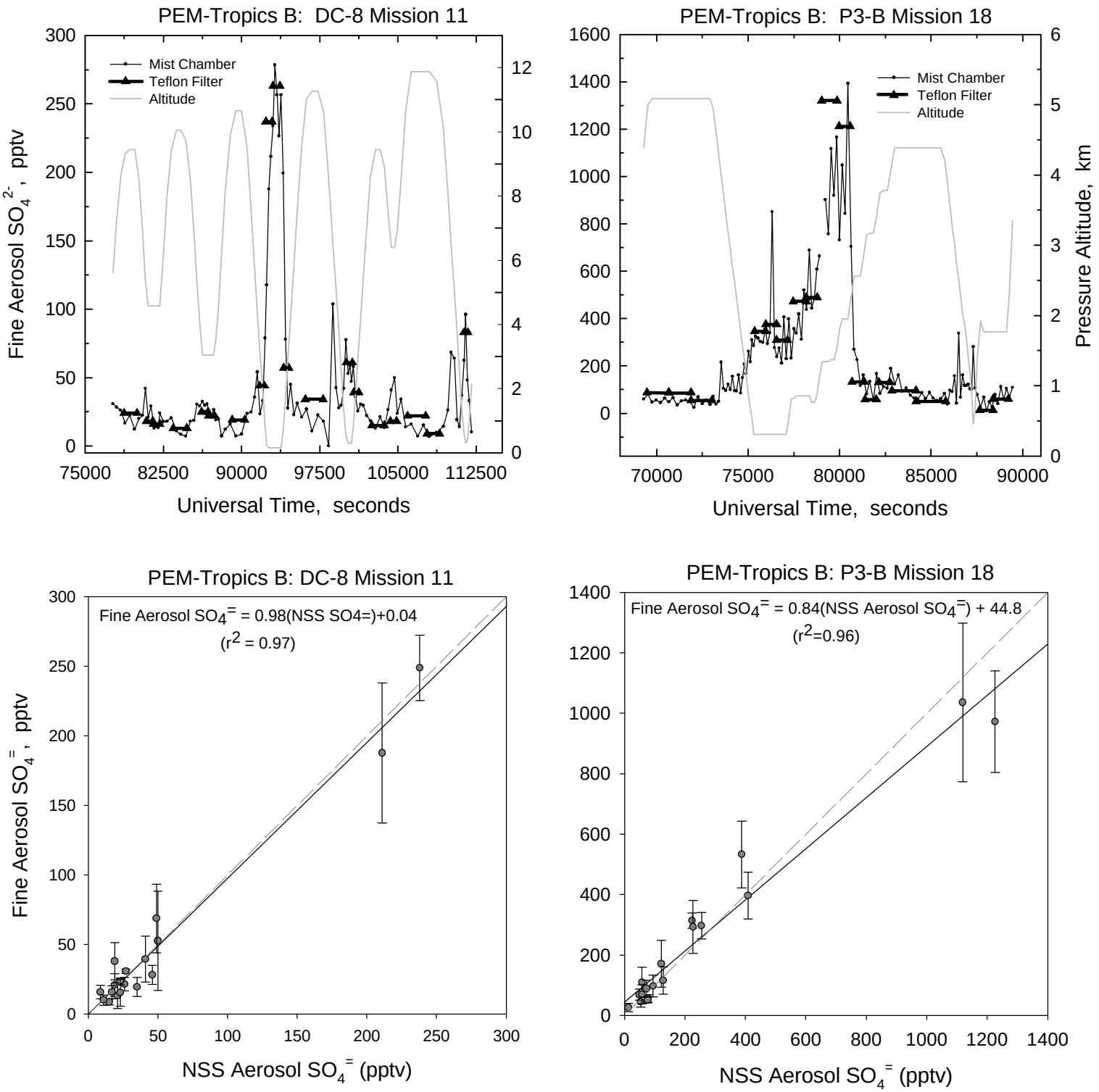
PEM-Tropics B: DC-8 Mission 11
Mist Chamber
Teflon Filter
Altitude
Fine Aerosol SO4 2-, pptv
Universal Time, seconds
PEM-Tropics B: P3-B Mission 18
Pressure Altitude, km
PEM-Tropics B: DC-8 Mission 11
Fine Aerosol SO4= = 0.98(NSS SO4=)+0.04
(r2 = 0.97)
Fine Aerosol SO4=, pptv
NSS Aerosol SO4= (pptv)
PEM-Tropics B: P3-B Mission 18
Fine Aerosol SO4= = 0.84(NSS Aerosol SO4=) + 44.8
(r2=0.96)

Figure 2.

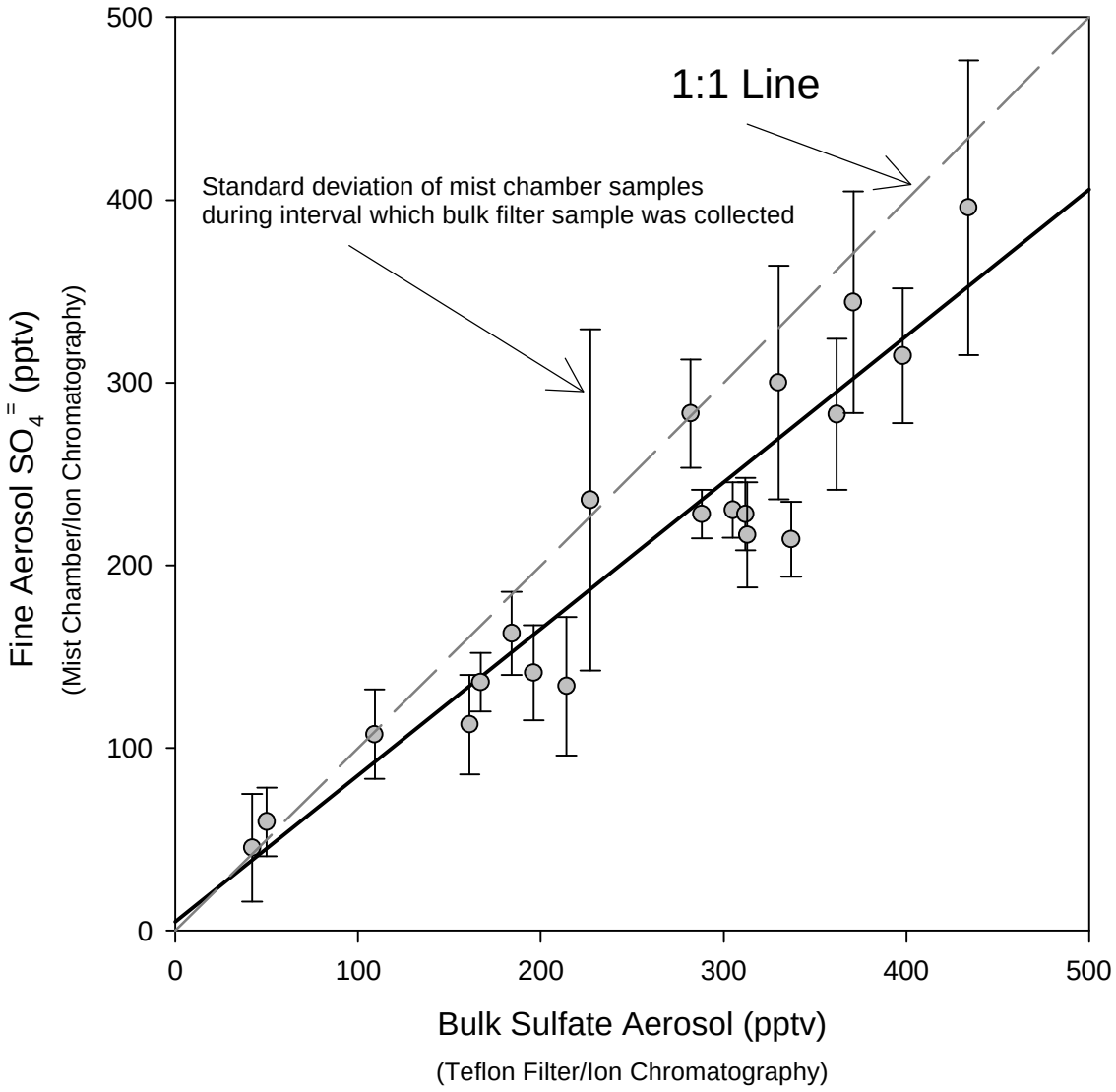
1:1 Line
Standard deviation of mist chamber samples
during interval which bulk filter sample was collected
Fine Aerosol $SO_4^=$ (pptv)
(Mist Chamber/Ion Chromatography)
Bulk Sulfate Aerosol (pptv)
(Teflon Filter/Ion Chromatography)
0
100
200
300
400
500

Figure 3.

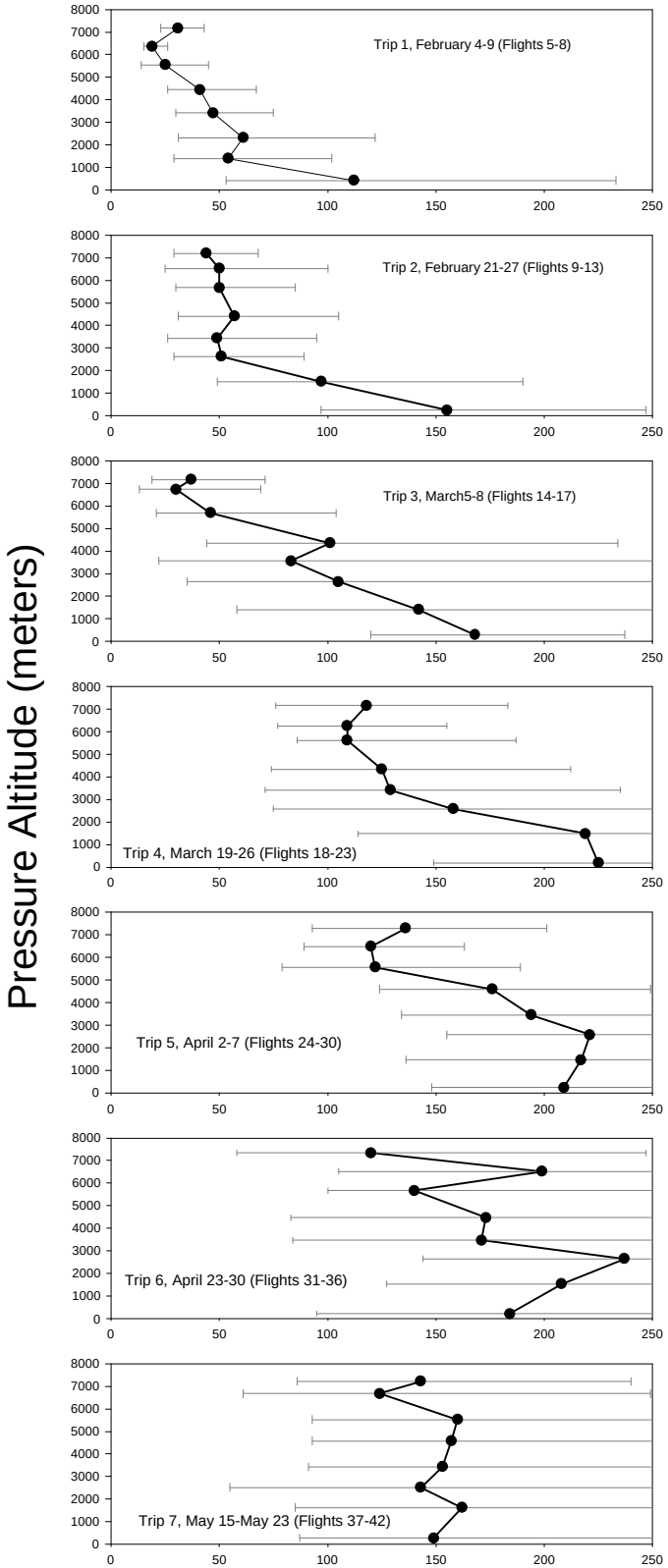
Pressure Altitude (meters)
Trip 1, February 4-9 (Flights 5-8)
Trip 2, February 21-27 (Flights 9-13)
Trip 3, March5-8 (Flights 14-17)
Trip 4, March 19-26 (Flights 18-23)
Trip 5, April 2-7 (Flights 24-30)
Trip 6, April 23-30 (Flights 31-36)
Trip 7, May 15-May 23 (Flights 37-42)
0 1000 2000 3000 4000 5000 6000 7000 8000
0 50 100 150 200 250
Fine Aerosol $SO_4^=$ (pptv)

Figure 4.

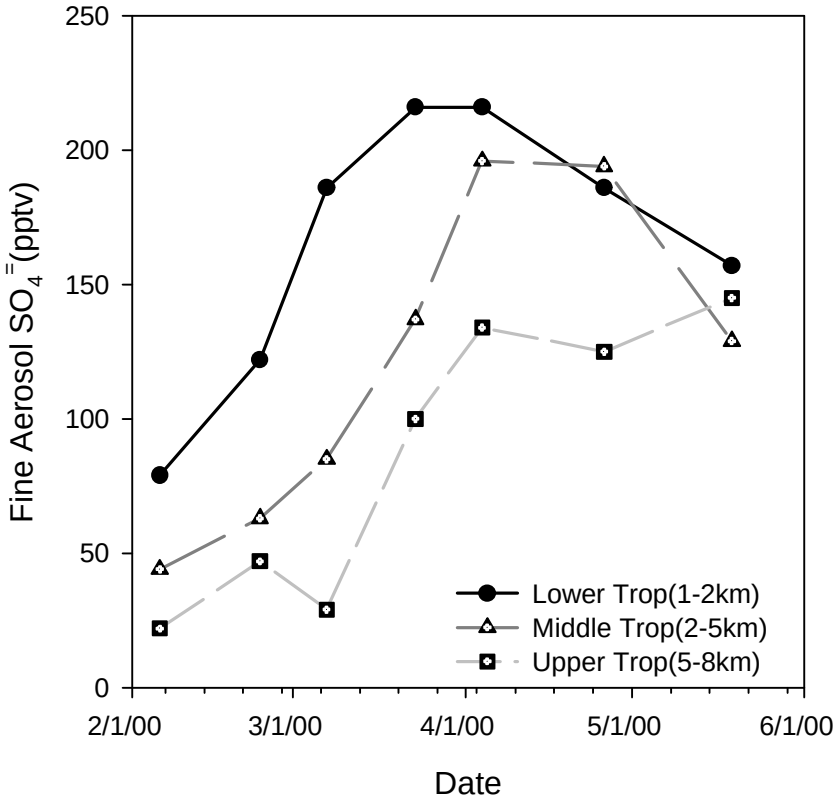
250
200
150
100
50
0
Fine Aerosol $SO_4^{=}$(pptv)
2/1/00
3/1/00
4/1/00
5/1/00
6/1/00
Date
Lower Trop(1-2km)
Middle Trop(2-5km)
Upper Trop(5-8km)

Figure 5.

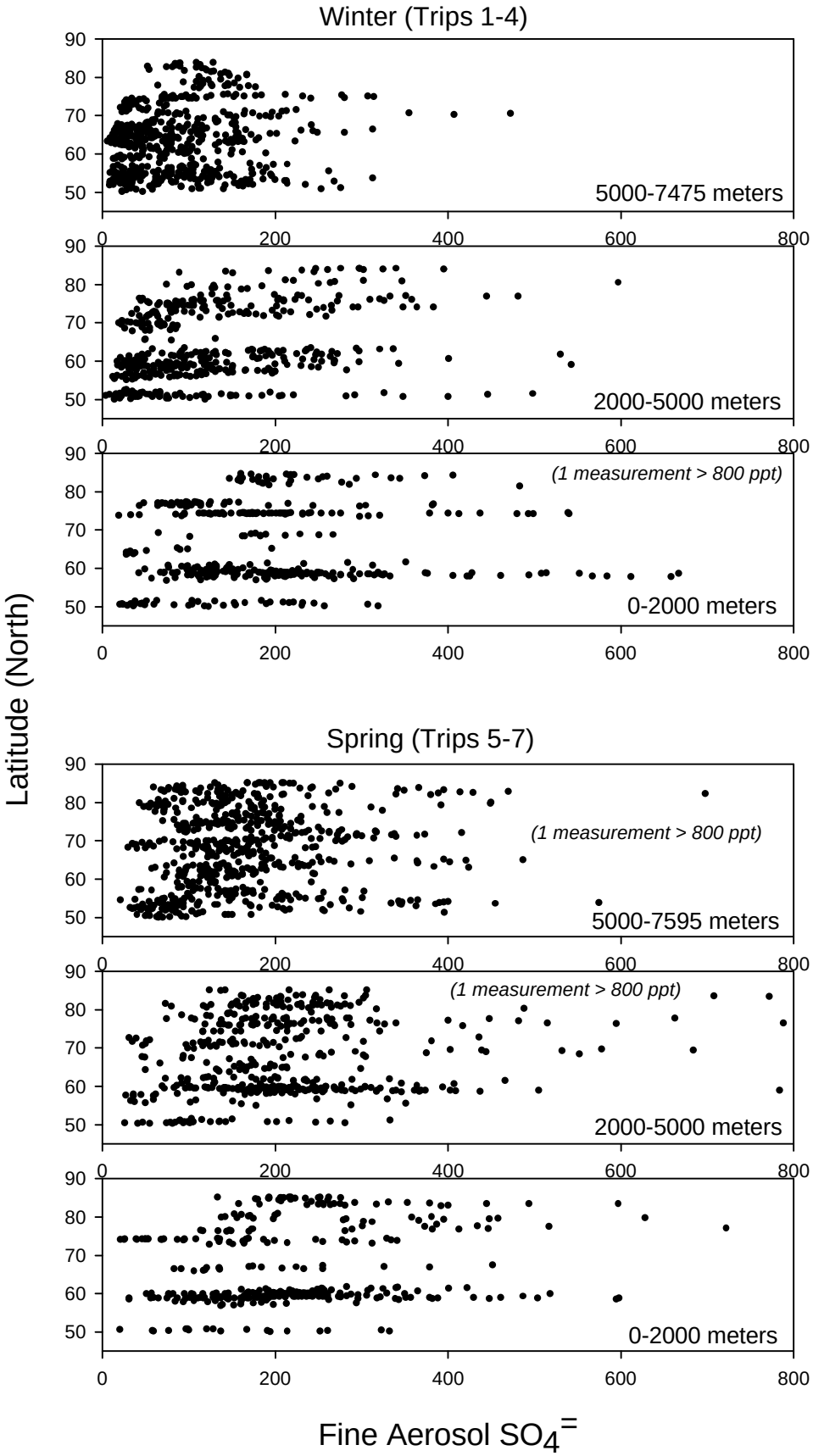
Winter (Trips 1-4)
5000-7475 meters
2000-5000 meters
(1 measurement > 800 ppt)
0-2000 meters
Spring (Trips 5-7)
(1 measurement > 800 ppt)
5000-7595 meters
(1 measurement > 800 ppt)
2000-5000 meters
0-2000 meters
Latitude (North)
Fine Aerosol $SO_4^=$

Figure 6.